

Perspectives on: Cyclic nucleotide microdomains and signaling specificity

## Mechanisms of cyclic AMP compartmentation revealed by computational models

Jeffrey J. Saucerman, Eric C. Greenwald, and Renata Polanowska-Grabowska

Department of Biomedical Engineering and Robert M. Berne Cardiovascular Research Center, University of Virginia, Charlottesville, VA 22908

### Introduction

Cyclic adenosine 3', 5'-monophosphate (cAMP) is a widely used biochemical messenger, transducing extracellular stimuli into a myriad of cellular responses. In the late 1970s, data emerged showing that hormone receptors acting via cAMP have distinct effects on cardiac function. At hormone levels where  $\beta$ -adrenergic and prostaglandin receptors induced similar changes in overall cAMP and PKA activity, only  $\beta$ -adrenergic receptors were found to increase left ventricular contractility, glycogen metabolism, and troponin I phosphorylation (Brunton et al., 1979; Hayes et al., 1979). This indicated that cAMP does not indiscriminately activate its downstream targets, but rather it acts in a context-dependent manner.

To explain the context-dependent specificity of cAMP, Brunton et al. (1981) proposed the compartmentation hypothesis, in which receptor-specific cAMP microdomains are distinctly coupled to cellular functions. Although this concept was initially quite controversial (Steinberg and Brunton, 2001), a variety of technologies has been developed over the past two decades that have enabled direct evidence of cAMP compartmentation. A key focus has become to understand the biochemical and biophysical mechanisms underlying cAMP compartmentation. Because of the limited ability to specifically perturb and measure all aspects of cAMP signaling experimentally, computational models have been developed to help understand how cAMP compartments are formed. Indeed, computational models are well suited for identifying biological mechanisms, predicting downstream consequences, and reducing the complexity of large datasets (Yang and Saucerman, 2011).

As the experimental efforts to measure and manipulate cAMP compartmentation have been well reviewed elsewhere (Steinberg and Brunton, 2001; Saucerman and McCulloch, 2006; Willoughby and Cooper, 2007; Karpen, 2014; Rich et al, 2014), this Perspective will concentrate on the specific insights into cAMP compartmentation

provided by computational models. Computational models have been used to evaluate a range of potential cAMP compartmentation mechanisms: localized cAMP synthesis, localized cAMP degradation, physical barriers to diffusion, cAMP buffering, cell shape, and cAMP export (see Fig. 1). After briefly summarizing key motivating experimental measurements, we will describe model predictions related to each of these potential mechanisms. We will then discuss future directions including necessary experimental validations of key model predictions and the incorporation of cAMP compartmentation into multi-scale computational models.

**Experimental measurements of cAMP compartmentation**  
*Biochemical approaches.* The initial measurements of cAMP compartmentation were performed by cellular fractionation and radioimmunoassay. Corbin et al. (1977) isolated particulate and soluble fractions of rabbit heart homogenates, finding that about half of the total cAMP content was bound to PKA regulatory subunit in the particulate fraction. Increasing cAMP synthesis or blocking its degradation caused disproportionate [cAMP] increases in the soluble fraction (Corbin et al., 1977). Although activation of both  $\beta$ -adrenergic and prostaglandin receptors increased soluble cAMP and PKA activity in heart homogenates, only  $\beta$ -adrenergic receptors elevated cAMP and PKA in the particulate fraction (Hayes et al., 1980) and triggered downstream increases in contractility and glycogen metabolism (Brunton et al., 1979). A limitation to these biochemical approaches is that they destroy the intact cellular environment, and particulate fractions contain a wide range of membranes, sarcomeres, and organelles.

*Electrophysiological approaches.* Creative use of patch-clamp electrophysiology allowed more direct measurement of cAMP compartmentation in live cells. Jurevicius

Correspondence to Jeffrey J. Saucerman: jsaucerman@virginia.edu

Abbreviations used in this paper: AC, adenylyl cyclase; AKAP, A kinase-anchoring protein; MRP, multidrug resistance protein; PDE, phosphodiesterase; PGE1, prostaglandin E1.

© 2014 Saucerman et al. This article is distributed under the terms of an Attribution-Noncommercial-Share Alike-No Mirror Sites license for the first six months after the publication date (see <http://www.rupress.org/terms>). After six months it is available under a Creative Commons License (Attribution-Noncommercial-Share Alike 3.0 Unported license, as described at <http://creativecommons.org/licenses/by-nc-sa/3.0/>).

and Fischmeister (1996) used a microperfusion system, finding that local application of the adenylyl cyclase (AC) agonist forskolin enhanced L-type  $\text{Ca}^{2+}$  currents globally, whereas locally applied  $\beta$ -adrenergic agonist isoproterenol produced only local elevations in L-type  $\text{Ca}^{2+}$  currents. These approaches were further enhanced by the use of CNG channels. Rich et al. (2000) used patch clamp of HEK293 cells expressing cAMP-sensitive CNG channels, finding that forskolin induced much higher submembrane [cAMP] than global [cAMP].

**Fluorescent biosensors.** A wide range of fluorescent biosensors for cAMP has been engineered. The first used fluorescein and rhodamine-labeled regulatory and catalytic subunits of PKA, where cAMP binding lead to a decrease in fluorescence resonance energy transfer between the fluorophores, allowing visualization of [cAMP] gradients induced by serotonin (Bacskai et al., 1993). Zacco et al. (2000) improved on this approach by fusing regulatory and catalytic subunits of PKA with cyan and yellow fluorescent proteins, creating a genetically encoded PKA-based biosensor. Their biosensor was used to visualize micrometer-scale cAMP gradients induced by  $\beta$ -adrenergic agonist in live cardiac myocytes (Zacco and Pozzan, 2002). Alternative cAMP biosensors have used conformational changes in the cAMP-binding protein Epac (DiPilato et al., 2004; Nikolaev et al., 2004) or the cAMP-binding domain of the hyperpolarization-activated CNG channel 2 (termed HCN2-camps) (Nikolaev et al., 2006).

#### Localized cAMP degradation

By far the most prominently recognized mechanism for cAMP compartmentation is localized cAMP degradation

by phosphodiesterases (PDEs) (Fig. 1 A) (Francis et al., 2011). Jurevicius and Fischmeister (1996) provided the first evidence of PDE-mediated cAMP compartmentation, showing that PDE inhibition allowed local  $\beta$ -adrenergic stimulation to enhance  $\text{Ca}^{2+}$  currents globally in frog ventricular myocytes. Inhibition of PDEs ablated compartment-specific cAMP dynamics and receptor-mediated cAMP gradients when using cAMP-sensitive CNG channels (Rich et al., 2001) or PKA-based fluorescent biosensors (Zacco and Pozzan, 2002).

Nearly all computational models have predicted a quantitatively important role of PDE-mediated cAMP degradation in the formation of cAMP gradients (see Table 1). The model developed by Rich et al. (2001) predicted that prostaglandin E1 (PGE1)-stimulated PDE activity was critical for quantitatively explaining the transient plasma membrane cAMP signals measured experimentally. A subsequent experimental and computational study from their group further demonstrated that the enhanced PDE activity was caused by PKA-mediated PDE phosphorylation (Rich et al., 2007), agreeing with previous experimental evidence of negative feedback by PKA on [cAMP] (Rochais et al., 2004). Saucerman et al. (2006) modeled cAMP and PKA signaling with image-based cardiac myocyte geometry, predicting that PDE regulated the magnitude of cytosolic cAMP/PKA gradients. Simulations with realistic neuronal geometries (Neves et al., 2008) have also explained how PDEs contribute to experimentally observed cAMP gradients between dendrites and the cell body (Bacskai et al., 1993).

The expression of multiple PDE isoforms and their localization to various cellular structures suggest that PDEs may regulate distinct cAMP compartments. In

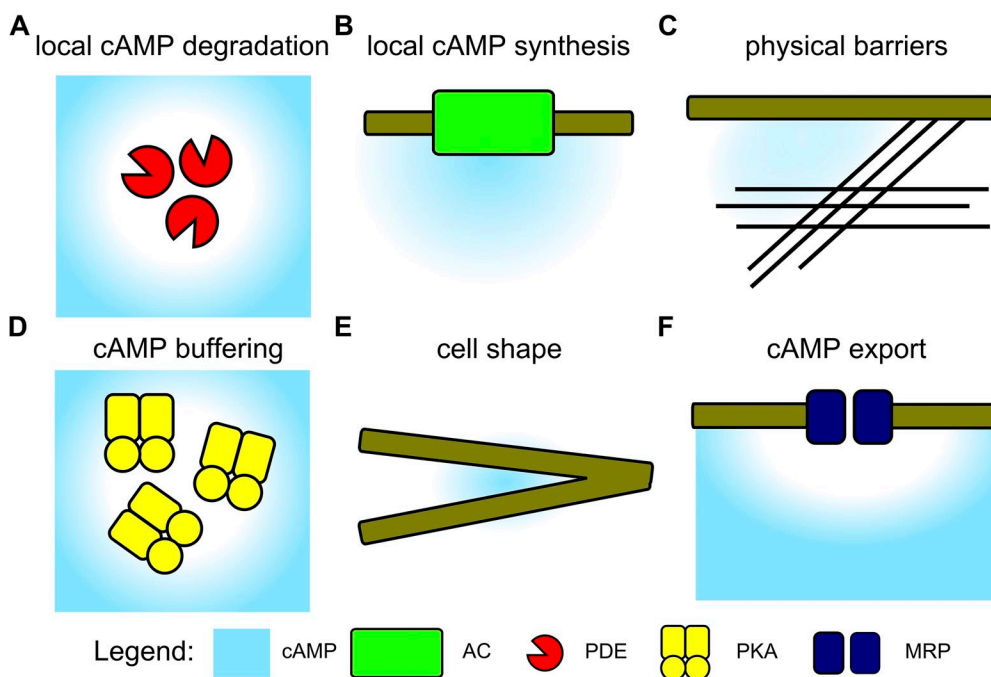


**Figure 1.** Predicted mechanisms of cAMP compartmentation. (A) PDEs can locally degrade cAMP to create gradients. (B) cAMP synthesis by AC can elevate local [cAMP]. (C) Physical barriers restrict cAMP diffusion. (D) cAMP binding to PKA can reduce the freely diffusing [cAMP]. (E) Cell shapes that alter the surface-to-volume ratio can alter the local balance of cAMP synthesis and degradation. (F) Export of cAMP from the cell by MRPs can decrease local [cAMP].

most cells, PDE3 and PDE4 are the dominant PDE isoforms for cAMP degradation (Francis et al., 2011). Although PDE3 contains membrane-binding domains and appears to target to intracellular membranes, PDE4 is primarily bound to A kinase-anchoring proteins (AKAPs) (Francis et al., 2011; Kapiloff et al., 2014) and localized in striated patterns, colocalized with either sarcomeric M-line or Z-lines (Mongillo et al., 2004). Measurement of cAMP signals using PKA-based fluorescence resonance energy transfer biosensors revealed that PDE4 dominates regulation of both basal and  $\beta$ -adrenergic-stimulated cAMP, whereas PDE3 dominated cAMP responses to forskolin in cardiac myocytes (Mongillo et al., 2004). Similarly, PDE4 plays a dominant role regulating subsarcolemmal cAMP, as measured by CNG channels expressed in cardiac myocytes (Rochais et al., 2004).

Several models have examined how PDE localization contributes to cAMP compartmentation. Saucerman et al. (2006) measured and modeled  $\beta$ -adrenergic-stimulated gradients of cAMP/PKA signaling between sarcolemma and cytosol, predicting that the measured time delays from sarcolemmal to cytosolic PKA activity were insensitive to PDE localization or mobility unless cAMP diffusion rates were slowed. Iancu et al. (2007) developed a multi-compartmental model of cAMP signaling in cardiac myocytes, including PDE2, PDE3, and PDE4 isoforms, and distinct sarcolemmal domains. Their model predicted that heterogeneous PDE localization (not the PDE isoform per se) was critical for maintaining cAMP gradients under basal and stimulated conditions (Iancu et al., 2007). This is a helpful model prediction because it is difficult to experimentally dissect PDE isoform localization from their distinct kinetic and regulatory properties. Heijman et al. (2011) further extended this model (as discussed below), predicting that PDE3 plays the dominant role in regulation of baseline caveolar and cytosolic [cAMP]. Chen et al. (2008) developed models with varying localization of PDEs, showing that

colocalization of PDEs with ACs provided optimal compartmentation. In contrast, they predicted that if PDEs were uniformly distributed, PDEs expressed at biochemically reasonable values would be insufficient to generate cAMP gradients (Chen et al., 2008).

Although most models of cAMP compartmentation have been deterministic (repetition of the same simulation gives the same results), Oliveira et al. (2010) developed a stochastic cAMP model to reflect the variability caused by small numbers of signaling molecules. Using this model, they predicted that PKA-mediated phosphorylation of cytosolic PDE4D creates a negative feedback critical for formation of submembrane cAMP microdomains in HEK293 cells (Oliveira et al., 2010), consistent with prior experiments (Rich et al., 2001; Terrin et al., 2006).

In summary, a wide range of experiments and models supports the key role of PDEs as necessary for generation of [cAMP] gradients. However, some of these models differ considerably in the extent to which PDE-mediated cAMP degradation is sufficient for [cAMP] gradients, or whether other mechanisms are required as well.

#### Localized cAMP synthesis

cAMP is synthesized by ACs from ATP. There are several types of ACs that differ in their distinct patterns of molecular regulation and tissue-specific expression (Hanoune and Defer, 2001; Willoughby and Cooper, 2007). Although all transmembrane ACs are activated by the binding of GTP-bound  $G_{sq}$  or the AC agonist forskolin, they differ in their molecular regulation and expression (Hanoune and Defer, 2001; Willoughby and Cooper, 2007). Soluble ACs have also been identified, which are activated by bicarbonate, and several bacteria have been shown to inject soluble ACs into mammalian cells as a toxin (Sayner et al., 2004). Early experimental studies suggested that hormone-specific cAMP compartments were generated by distinct coupling of receptors and G proteins with

TABLE 1  
*Comparison of computational models that have predicted mechanisms contributing to cAMP compartmentation*

| Model                  | Cell type        | cAMP synthesis | cAMP degradation | Physical barriers | cAMP buffers | cAMP export | Cell shape |
|------------------------|------------------|----------------|------------------|-------------------|--------------|-------------|------------|
| Rich et al., 2000      | HEK293           |                |                  | X                 |              |             |            |
| Rich et al., 2001      | HEK293           |                | X                | X                 |              |             |            |
| Rich et al., 2007      | HEK293           |                | X                | X                 |              |             |            |
| Oliveira et al., 2010  | HEK293           |                | X                |                   |              |             |            |
| Xie et al., 2011       | T84              |                | X                | X                 |              | X           |            |
| Sample et al., 2012    | HEK293           | X              | X                | X                 |              |             |            |
| Saucerman et al., 2006 | Cardiac myocyte  | X              | X                | X                 | X            |             |            |
| Iancu et al., 2007     | Cardiac myocyte  | X              | X                | X                 |              |             |            |
| Heijman et al., 2011   | Cardiac myocyte  | X              | X                | X                 |              |             |            |
| Neves et al., 2008     | Neuron           |                | X                |                   |              |             | X          |
| Chen et al., 2009      | Neuron           |                | X                |                   |              |             | X          |
| Feinstein et al., 2012 | Endothelial cell | X              | X                | X                 | X            |             | X          |
| Chen et al., 2008      | Idealized        | X              | X                |                   |              |             |            |

subpopulations of transmembrane ACs in specific compartments (Brunton et al., 1981). Localization of different AC isoforms with distinct regulators of cAMP synthesis (e.g.,  $\beta_1$ -adrenergic receptors,  $\beta_2$ -adrenergic receptors,  $G_s$ , PKA) at caveolae (Rybin et al., 2000; Ostrom et al., 2001) or on specific AKAP complexes (Kapiloff et al., 2014) has been shown to be a potential molecular mechanism for the formation of specific cAMP microdomains (Fig. 1 B).

CNG channels and fluorescent biosensors are frequently used to measure localized cAMP synthesis by subsets of ACs. Rochais et al. (2004) expressed CNG channels in rat ventricular myocytes to compare the responses to  $\beta$ -adrenergic and AC agonists, finding that  $\beta$ -adrenergic receptors activate only  $\sim 25\%$  of ACs. This measurement quantitatively validated predictions from a previous computational model of  $\beta$ -adrenergic/cAMP/ $Ca^{2+}$  signaling (Saucerman et al., 2003). Rochais et al. (2006) went on to compare subsarcolemmal cAMP signals and changes in L-type  $Ca^{2+}$  currents, finding receptor-specific signatures in response to isoproterenol, glucagon, and PGE1. As an alternative approach, the HCN2-camps cAMP biosensor showed that local  $\beta_1$ -AR-elicited cAMP signals propagated globally, whereas cAMP signals generated by local  $\beta_2$ -AR stimulation remained localized (Nikolaev et al., 2006). This approach was elegantly extended to also include scanning ion conductance, allowing delivery of  $\beta_1$ -AR and  $\beta_2$ -AR stimuli specifically to t-tubules or outer sarcolemma (Nikolaev et al., 2010). Their data indicated that  $\beta_2$ -AR-mediated cAMP synthesis is normally limited to t-tubules, but these receptors redistribute to outer sarcolemma in heart failure (Nikolaev et al., 2010). The Zaccolo group tethered Epac-based cAMP sensors to type I and type II PKA regulatory subunits and assessed receptor-specific cAMP signals in these compartments (Di Benedetto et al., 2008). These experiments revealed higher cAMP in the type I PKA compartment with  $\beta$ -AR stimulation, whereas glucagon and PGE1 generated higher [cAMP] in the type II PKA compartment (Di Benedetto et al., 2008).

The Harvey group has developed computational models that examine the distinct cAMP microdomains induced by stimulus-specific local cAMP synthesis. Iancu et al. (2007) extended models of  $\beta$ -adrenergic/cAMP signaling in cardiac myocytes (Saucerman et al., 2003, 2006) by incorporating caveolar, extra-caveolar membrane, and cytosolic compartments, each with experimentally based distributions of receptors ( $\beta_1$ -AR and muscarinic) and AC isoforms (Iancu et al., 2007). This model predicted that baseline caveolar [cAMP] is considerably below cytosolic [cAMP], preventing constitutive activation of caveolar PKA. They used this model to predict localized cross talk between  $\beta_1$ -adrenergic and  $M_2$ -muscarinic receptors.  $M_2$ -muscarinic receptors were predicted to inhibit  $\beta_1$ -AR responses in caveolae but enhance cAMP synthesis outside caveolae (Iancu et al., 2007), leading to a quantitative explanation for the

intriguing acetylcholine rebound effect (Belevych et al., 2001). Their group subsequently compared the PKA-based cAMP biosensor with a cytosolic Epac-based sensor, allowing improved validation of their previous model predictions of elevated cytosolic [cAMP] and muscarinic stimulation of cytosolic [cAMP] increases (Iancu et al., 2008). Later, this compartmental model was extended by adding  $\beta_2$ -ARs, PKA, and downstream signaling (Heijman et al., 2011). Heijman et al. (2011) performed a series of virtual knockouts and perturbations, predicting  $\beta_1$ -AR-versus  $\beta_2$ -AR-specific local cAMP signals and distinct roles of AC5/6 and AC4/7 regulating caveolar/cytosolic [cAMP] and extracaveolar [cAMP], respectively.

New experimental techniques for controlling local cAMP synthesis have provided additional insights into mechanisms of cAMP compartmentation. Saucerman et al. (2006) found that receptor-stimulated cAMP synthesis generated PKA activity gradients between plasma membrane and adjacent cytosol, whereas cAMP released by local uncaging in the cytosol had a much larger range of action. These measurements were quantitatively explained using their computational models (Saucerman et al., 2006). ACs have also been reengineered to provide further control of local cAMP synthesis. To explain the paradoxical effects of transmembrane versus soluble ACs on endothelial barrier function (Sayner et al., 2004), Sayner et al. (2006) used a cytosolic-targeted AC mutant, finding that indeed the membrane versus cytosolic location of cAMP synthesis determined whether cAMP increased or decreased barrier function.

Development of genetically targetable and bicarbonate-sensitive soluble AC constructs allowed analysis of how cAMP and PKA activity gradients depend on the subcellular location of cAMP synthesis (Sample et al., 2012). They found that cAMP synthesis at either plasma membrane or nucleus generated high local [cAMP] but lower distal [cAMP] in HEK293 cells. Further, nuclear PKA activity was rapidly activated by nuclear cAMP, in contrast to computational models based on the classical paradigm of slow nuclear import of PKA catalytic subunit. Iteration between alternative computational models and cAMP biosensor experiments with localized cAMP synthesis allowed inference of a resident pool of PKA holoenzyme bound to AKAPs and insulated from global cAMP by tethered PDE4 (Sample et al., 2012). A unique aspect of the modeling approach in this study was the iterative rejection and revision of computational models together with new experiments to identify a new cAMP/PKA microdomain.

Overall, several computational models have been established to evaluate the impact of localized cAMP synthesis on generation of [cAMP] gradients. Despite a variety of interesting experimental studies showing receptor-specific cAMP microdomains, it is important to remember that localized cAMP synthesis may not fully explain functional differences. Such differences

could also be related to the magnitude or kinetics of the stimulus, PDE-mediated cAMP degradation, or cAMP-independent pathways. Although several of the experimentally observed receptor-specific cAMP microdomains discussed above are not yet accurately predicted, these models will serve as a useful framework for future experimental and computational studies. Such complexities further indicate the need for computational models in this area.

#### Physical barriers to cAMP diffusion

Although a wide range of experimental studies have clearly demonstrated that cAMP gradients are regulated by localized cAMP synthesis and degradation, even the simplest (and most elegant) computational models indicated that this picture may be incomplete. Rich et al. (2000) presented a simple analytical model of cAMP diffusion from a single AC protein. This analysis demonstrated that in contrast to the substantial gradients in  $\text{Ca}^{2+}$  in the vicinity of  $\text{Ca}^{2+}$  channels (Fischmeister and Horackova, 1983), biochemically measured rates of AC activity are insufficient alone (by a factor of  $>100$ ) to generate meaningful cAMP gradients (Rich et al., 2000). A similar finding was obtained even when extending analytical models with localized PDEs (Chen et al., 2008). Indeed, only models with physical barriers to cAMP diffusion between plasma membrane and cytosol could predict experimentally measured distinct local cAMP gradients induced by forskolin or PGE1 (Rich et al., 2000, 2001).

Several computational models were consistent with this concept of restricted cAMP diffusion (Fig. 1 C). Prediction of experimentally measured time delays between membrane and cytosolic PKA activity required substantially reduced cAMP diffusion rates (by  $>100\times$ ) (Saucerman et al., 2006). Simulations of PKA gradients generated by local cAMP uncaging predicted that cytosolic cAMP diffusion may also be restricted but to a lesser degree (Saucerman et al., 2006). Likewise, the Iancu et al. (2007, 2008) models predicted that low basal [cAMP] in caveolae and compartment-specific cross talk between  $\beta 1$ -adrenergic and muscarinic signaling depended critically on restricted cAMP diffusion between membrane compartments and cytosol. Similar conclusions were obtained in models of distinct cAMP microdomains regulated by  $\beta 1$ -AR and  $\beta 2$ -AR in cardiac myocytes (Heijman et al., 2011). The role of restricted cAMP diffusion has also been tested in simulations with realistic geometries of endothelial cells (Feinstein et al., 2012). cAMP synthesis and degradation rates were varied over wide ranges, demonstrating that unless AC/PDE-mediated cAMP synthesis/degradation fluxes were highly elevated (by  $>100\times$ ), cAMP gradients required restricted cAMP diffusion (Feinstein et al., 2012).

However, some computational models have indicated that a reduction in the diffusion coefficient is not

required for cAMP gradients. The previously described models of cAMP gradients in realistic neuron geometries (Neves et al., 2008) used an unrestricted cAMP diffusion coefficient of  $200 \mu\text{m}^2/\text{s}$ . cAMP gradients in these cells relied on a high PDE activity and additional features of cell shape as described below in Regulation of cAMP gradients by cell shape. The stochastic models of Oliveira et al. (2010) predicted that local cAMP synthesis together with broadly distributed and PKA-sensitive cAMP degradation were sufficient to generate experimentally observed cAMP gradients in HEK293 cells. The difference in this model may be caused either by the stochastic nature of the model or the assumed  $>500$ -fold higher cAMP synthesis and degradation rates ( $V_{\text{max PDE}}, 55\text{--}348 \mu\text{M s}^{-1}$ ) than had been measured biochemically and included in the other models (Rich et al., 2000, 2001; Saucerman et al., 2006; Feinstein et al., 2012) (see Table 2).

Although prediction of physical barriers restricting cAMP diffusion was certainly a surprising result (Rich et al., 2000), evidence of restricted diffusion of other small molecules has been reported as well. Fluorescent imaging of  $[\text{Na}^+]$  in ventricular myocytes with local  $\text{Na}^+/\text{K}^+$  pump inhibition identified substantial intracellular  $[\text{Na}^+]$  gradients, with an effective diffusion coefficient  $\sim 100$ -fold lower than in aqueous solutions (Despa et al., 2004). The distribution of 3–100-nm gold nanoparticles injected into permeabilized cardiac myocytes indicated substantial physical barriers both in the cytosol and subcellular spaces such as the dyadic cleft and nucleus (Parfenov et al., 2006). Restricted diffusion of nucleotides closely related to cAMP has been found as well. Jephthina et al. (2011) measured the kinetics of metabolic respiration in cardiac myocytes in response to locally applied ADP, finding delays in response that could only be explained by modeling diffusional obstacles. Correlation microscopy has been applied to fluorescently labeled ATP, measuring effective diffusion coefficients of  $\sim 4 \mu\text{m}^2/\text{s}$  with periodic physical barriers of  $\sim 1\text{-}\mu\text{m}$  spacing (Illaste et al., 2012).

Overall, most computational models based on biochemically measured rates of cAMP synthesis and degradation indicate that physical barriers are necessary to predict physiological cAMP gradients. However, the identity of these physical barriers is unknown, with possibilities including endoplasmic/sarcoplasmic membranes (Rich et al., 2000), cortical actin cytoskeleton, and myofibrillar proteins in muscle cells. Although gaps in actin cytoskeleton may be considerably larger than cAMP, it has been noted that actin networks form gels that considerably decrease local viscosity (Luby-Phelps et al., 1986). A major challenge remains to identify and experimentally perturb physical barriers to test these model predictions without unintentionally manipulating other variables such as AC/PDE activity and localization.

### Restricted diffusion caused by cAMP buffering

In addition to physical barriers, cAMP-binding proteins may bind cAMP to restrict cAMP diffusion (Fig. 1 D). PKA is the most likely candidate cAMP buffer, as it binds cAMP with higher affinity or is present in larger quantities than Epac, PKG, or CNG channels (Rich et al., 2001; Poppe et al., 2008). Early biochemical studies indicated that an appreciable fraction of total cAMP is bound to PKA, even in unstimulated conditions (Beavo et al., 1974; Corbin et al., 1977). The model of  $\beta$ -adrenergic signaling developed by Saucerman et al. (2003) accounted for both free and bound cAMP, predicting that PKA buffers the total [cAMP] by shielding it from PDE-mediated degradation. cAMP buffering was hypothesized to stabilize cAMP in the region of maximal PKA sensitivity (Saucerman et al., 2003). cAMP buffering by PKA was later revisited in the context of localized cAMP release, where cAMP buffering was predicted to contribute to cytosolic cAMP/PKA activity gradients (Saucerman et al., 2006). cAMP buffering has also been

predicted to contribute to cAMP gradients in endothelial cells, although primarily in cases where cAMP buffering was elevated or coupled with physical barriers (Feinstein et al., 2012). Although cAMP buffering has been predicted to restrict cAMP diffusion in some cases, it should be noted that PKA's buffering capacity for cAMP ( $\sim 1.2 \mu\text{mol/L}$  cytosol; Corbin et al., 1977; Saucerman et al., 2003) is much lower than the buffering capacity for  $\text{Ca}^{2+}$ . Direct experiments that manipulate cAMP buffering while measuring cAMP gradients are needed to validate these model predictions and resolve this issue.

### Regulation of cAMP gradients by cell shape

The first direct measurements of receptor-mediated cAMP gradients showed elevated [cAMP] in neuronal dendrites, with lower [cAMP] in the cell body (Bacskai et al., 1993). Bacskai et al. (1993) suggested that one of the simplest explanations for these cAMP gradients was the difference in surface-to-volume ratio; dendrites with large surface-to-volume ratio would be enriched in

TABLE 2  
Key numbers for cAMP compartmentation

| Biological parameters             | Values   |
|-----------------------------------|--|
| Length scales                     | Adult cardiac myocyte, 120 $\mu\text{m}$ ; HEK293, 16 $\mu\text{m}$ ; endothelial cell, 40 $\mu\text{m}$ ; neuronal dendrite length/width, 100/3 $\mu\text{m}$ ; cAMP hydrodynamic radius, 1.4 nm  |
| Concentrations                    | Free cAMP, 0.1–5 $\mu\text{M}$ ; type I PKA, 0.59 $\mu\text{M}$ ; type II PKA, 25 nM; Saucerman et al., 2003; CNG channels, 40 nM; Rich et al., 2001   |
| Diffusion coefficients for cAMP   | Aqueous solution, 444 $\mu\text{m}^2 \text{s}^{-1}$ ; Dworkin and Keller, 1977; CHO cell, 487 $\mu\text{m}^2 \text{s}^{-1}$ ( $v = 40 \mu\text{m s}^{-1}$ ); Nikolaev et al., 2004; Cardiac myocyte, 136 $\mu\text{m}^2 \text{s}^{-1}$ ( $v = 16 \mu\text{m s}^{-1}$ ); Nikolaev et al., 2006. Physical barriers between membrane and cytosol: 0.5 $\mu\text{m}^2 \text{s}^{-1}$ over 1 $\mu\text{m}$ ; Rich et al., 2000; 2 $\mu\text{m}^2 \text{s}^{-1}$ over 2.5 $\mu\text{m}$ ; Saucerman et al., 2006   |
| Rate constants                    |  |
| <b>AC:</b>                        | kcat-AC, 12–60 $\text{s}^{-1}$ ; Rich et al., 2000; 8.5 $\text{s}^{-1}$ ; Saucerman et al., 2003<br>20 $\text{s}^{-1}$ ; Feinstein et al., 2012;<br>Vmax-AC: cardiac myocyte, 0.1–0.4 $\mu\text{M s}^{-1}$ ; Saucerman et al., 2003, 2006; endothelial cell, 0.14 $\mu\text{M s}^{-1}$ ; Feinstein et al., 2012; HEK293, 0.13 $\mu\text{M s}^{-1}$ ; Rich et al., 2001   |
| <b>PDE:</b>                       | kcat-PDE3: 3.5 $\text{s}^{-1}$ ; kcat-PDE4: 5 $\text{s}^{-1}$ ; Saucerman et al., 2004; Vmax-PDE: cardiac myocyte, 0.2–0.4 $\mu\text{M s}^{-1}$ ; Saucerman et al., 2003; endothelial cell, 0.3 $\mu\text{M s}^{-1}$ ; Feinstein et al., 2012; neuron, 3.4 $\mu\text{M s}^{-1}$ ; Neves et al., 2008   |
| <b>MRP4:</b>                      | k-MRP4: $10^{-4}$ to $10^{-3} \text{s}^{-1}$ ; Cheepala et al., 2013   |
| Back-of-the-envelope calculations | <b>Time for cAMP to diffuse across a cell:</b><br><b>Cardiac myocyte:</b><br>Aqueous diffusion rate: 4 s<br>Cytosolic diffusion rate: 13 s<br><b>HEK293:</b><br>Aqueous diffusion rate: 0.07 s<br>Time for cAMP to diffuse from membrane to cytosol in cardiac myocyte: 1.6 s<br>Time to degradation of cAMP by PDE: 0.5–50 s<br><b>Distance for cAMP diffusion before degradation by PDE:</b><br>Aqueous diffusion rate: $\text{sqrt}(2 \cdot 444 \cdot t_0) = 21\text{--}210 \mu\text{m}$<br>Cardiac myocyte cytosol: 12–117 $\mu\text{m}$<br>Restricted diffusion cardiac myocyte = 1–10 $\mu\text{m}$<br>CHO cytosol: 22–220 $\mu\text{m}$ |

Rate constants were obtained from example models as determined from biochemical experiments. Diffusion calculations performed using the solution to the 1-D diffusion equation,  $\langle x^2 \rangle = 2Dt$ , where  $\langle x^2 \rangle$  is the mean-squared distance traveled,  $D$  is the diffusion coefficient, and  $t$  is time (Codling et al., 2008). Using a linear approximation of cAMP degradation by PDE, the time to degradation was calculated by  $t_{deg} = [cAMP]/V_{max} - PDE$ . The time to degradation was then used in the 1-D diffusion equation to determine the diffusion distance before degradation. Note that the range of action of cAMP is predicted to increase with increasing [cAMP] and decrease with increasing [PDE].

transmembrane AC but contain less cytosolic PDE (Fig. 1 E). 15 years later, Neves et al. (2008) performed similar measurements with fluorescent protein-based cAMP biosensors, again finding elevated [cAMP] in dendrites compared with cell body. They built a computational model of local cAMP signaling, predicting that indeed the compartmental differences in surface-to-volume ratio were sufficient to quantitatively predict cAMP gradients, without decreasing the cAMP diffusion coefficient (Neves et al., 2008). Chen et al. (2009) further developed models of neurons with idealized geometries, deriving analytical expressions relating the length and width of the dendrite, cAMP degradation rate, and [cAMP] gradient magnitudes. The models of Feinstein et al. (2012) examined how cAMP gradients may be affected by physiological variation in endothelial cell shape. They found that although surface-to-volume ratios typical of endothelial cell geometries were insufficient to generate cAMP gradients alone, cell shape did significantly enhance the sensitivity to other mechanisms such as restricted cAMP diffusion (Feinstein et al., 2012).

In summary, several computational models predict that subcellular geometries with high surface-to-volume ratios enhance cAMP gradients, primarily when those geometries are at least 5  $\mu\text{m}$ . This indicates that surface-to-volume ratio may be insufficient to explain cAMP gradients in nanometer-scale compartments such as dyadic clefts or caveolae. Experiments that manipulate cell shape will be needed to test these model predictions. But like predictions for physical barriers, it may be difficult to perform direct perturbations without also changing other key variables.

#### cAMP export

cAMP can also be eliminated from the cell by export via multidrug resistance proteins (MRPs) (see Fig. 1 F). Although MRP-mediated cAMP export rates are very low ( $2 \times 10^{-3} \text{s}^{-1}$ ) relative to overall PDE activities with small effects on global [cAMP] (Cheepala et al., 2013), several studies have shown that inhibition of MRP can considerably elevate submembrane [cAMP] (Li et al., 2007; Xie et al., 2011). However, these studies are complicated because pharmacologic MRP inhibitors block PDE activity, whereas genetic MRP knockdown can alter PDE expression (Xie et al., 2011). Models extended to include MRP-mediated cAMP export demonstrated that modulation of local but not global cAMP by MRP4 required a membrane compartment with highly restricted cAMP diffusion, low PDE, and high MRP4 (Xie et al., 2011).

#### Conclusions and future directions

The study of cAMP compartmentation has undergone a series of paradigm shifts enabled by new technologies, from inference by functional measurements to indirect biochemical measurements, to direct measurements in live cells. Since the advent of cAMP-sensitive CNG

channels and fluorescent biosensors, considerable experimental efforts have been focused on understanding the mechanisms underlying cAMP gradients. Of these potential mechanisms, local cAMP degradation by PDEs has been best characterized because of the availability of specific pharmacologic and genetic perturbations. Reasonably strong experimental support has also been provided for the role of local cAMP synthesis, although better targeted tools for measuring and perturbing local cAMP signals (e.g., at AKAPs, caveolae) are still needed to explain several receptor-specific responses. A variety of computational models have been developed to quantitatively explain how previously measured cAMP microdomains are regulated by local cAMP synthesis and degradation (Table 1). Models have also been used to quantitatively explain experimentally observed regulation of cAMP microdomains by cell shape and cAMP export.

In addition to their explanatory power, in several cases *de novo* predictions from computational models have been validated in subsequent experiments. Early models of  $\beta$ -adrenergic signaling (Saucerman et al., 2003) accurately predicted that  $\beta$ 1-AR activate only a subpopulation of ACs (Rochais et al., 2004), restricting amplification of the pathway. Model predictions of cAMP as the rate-limiting step in  $\beta$ -adrenergic signaling and predictions of time delays between membrane and cytosolic cAMP signals (Saucerman et al., 2006) were also validated in separate experiments (Leroy et al., 2008). A model of  $\beta$ -adrenergic/ $M_2$ -muscarinic receptor cross talk (Iancu et al., 2007) predicted the subsequently validated cytosolic [cAMP] signals underlying the rebound effect caused by transient acetylcholine (Iancu et al., 2008). As a last example, models of nuclear cAMP and PKA activity correctly predicted a distinctly regulated nuclear PKA-AKAP-PDE4 complex in HEK293 cells (Sample et al., 2012).

*Experimental validation of predicted compartmentation mechanisms.* Additional experimental studies are needed to directly validate novel predictions of other cAMP compartmentation mechanisms. Experimental validation of the role of cAMP buffering may be feasible by the careful use of specific cAMP analogues (Poppe et al., 2008). In contrast, the identification and specific perturbation of physical barriers modulating cAMP compartmentation appears considerably more challenging. Further experimental validations regarding the role of cell shape are also required, including perturbations that modulate cell shape dynamically and examination of additional cellular structures. For example, PKA activity gradients have been observed at the leading edge of migrating cells (Lim et al., 2008), which has a much higher surface-to-volume ratio than at the rear.

*Modeling functional consequences of cAMP compartmentation.* In addition to inferring biophysical mechanisms,

computational models are also valuable for integrating distinct biological processes and predicting the multi-scale consequences of mechanistic perturbations (Yang and Saucerman, 2011). For example, a model coupling  $\beta$ -adrenergic signaling, cellular excitation–contraction coupling, and 3-D electrophysiology across the heart wall (Saucerman et al., 2004) was able to mechanistically predict how human mutations that disrupts a PKA–AKAP channel complex lead to T-wave abnormalities subsequently measured in patients with long QT syndrome 1 (Darbar et al., 2005). Heijman et al. (2011) also examined the impact of localized cAMP/PKA signaling on cardiac physiology, predicting in detail how  $\beta$ 1- and  $\beta$ 2-adrenergic stimuli and cross talk with  $\text{Ca}^{2+}$ /calmodulin kinase II lead to distinct regulation of action potentials and  $\text{Ca}^{2+}$  transients. Neves et al. (2008) predicted and then experimentally validated that cAMP gradients in neurons help drive gradients in downstream MAPK signaling related to synaptic plasticity. Greater use of integrative, multi-scale models would aid the understanding of cAMP compartmentation in health and disease but also enable in silico design of novel therapeutics based on manipulation of local cAMP signals.

This Perspectives series includes articles by [Karpen](#), [Kapiloff et al.](#), [Rich et al.](#), and [Conti et al.](#)

This work was supported by the National Institutes of Health (grants HL094476, HL05242, and GM007055) and a National Science Foundation CAREER grant (1252854).

Olaf S. Andersen served as editor.

## REFERENCES

- Bacskai, B.J., B. Hochner, M. Mahaut-Smith, S.R. Adams, B.K. Kaang, E.R. Kandel, and R.Y. Tsien. 1993. Spatially resolved dynamics of cAMP and protein kinase A subunits in Aplysia sensory neurons. *Science*. 260:222–226. <http://dx.doi.org/10.1126/science.7682336>
- Beavo, J.A., P.J. Bechtel, and E.G. Krebs. 1974. Activation of protein kinase by physiological concentrations of cyclic AMP. *Proc. Natl. Acad. Sci. USA*. 71:3580–3583. <http://dx.doi.org/10.1073/pnas.71.9.3580>
- Belevych, A.E., C. Sims, and R.D. Harvey. 2001. ACh-induced rebound stimulation of L-type  $\text{Ca}^{2+}$  current in guinea-pig ventricular myocytes, mediated by Gbetagamma-dependent activation of adenylyl cyclase. *J. Physiol.* 536:677–692. <http://dx.doi.org/10.1111/j.1469-7793.2001.00677.x>
- Brunton, L.L., J.S. Hayes, and S.E. Mayer. 1979. Hormonally specific phosphorylation of cardiac troponin I and activation of glycogen phosphorylase. *Nature*. 280:78–80. <http://dx.doi.org/10.1038/280078a0>
- Brunton, L.L., J.S. Hayes, and S.E. Mayer. 1981. Functional compartmentation of cyclic AMP and protein kinase in heart. *Adv. Cyclic Nucleotide Res.* 14:391–397.
- Cheepala, S., J.S. Hulot, J.A. Morgan, Y. Sassi, W. Zhang, A.P. Naren, and J.D. Schuetz. 2013. Cyclic nucleotide compartmentalization: contributions of phosphodiesterases and ATP-binding cassette transporters. *Annu. Rev. Pharmacol. Toxicol.* 53:231–253. <http://dx.doi.org/10.1146/annurev-pharmtox-010611-134609>
- Chen, W., H. Levine, and W.J. Rappel. 2008. A mathematical analysis of second messenger compartmentalization. *Phys. Biol.* 5:046006. <http://dx.doi.org/10.1088/1478-3975/5/4/046006>
- Chen, W., H. Levine, and W.J. Rappel. 2009. Compartmentalization of second messengers in neurons: a mathematical analysis. *Phys. Rev. E Stat. Nonlin. Soft Matter Phys.* 80:041901. <http://dx.doi.org/10.1103/PhysRevE.80.041901>
- Codling, E.A., M.J. Plank, and S. Benhamou. 2008. Random walk models in biology. *J. R. Soc. Interface*. 5:813–834. <http://dx.doi.org/10.1098/rsif.2008.0014>
- Corbin, J.D., P.H. Sugden, T.M. Lincoln, and S.L. Keely. 1977. Compartmentalization of adenosine 3':5'-monophosphate and adenosine 3':5'-monophosphate-dependent protein kinase in heart tissue. *J. Biol. Chem.* 252:3854–3861.
- Darbar, D., D.M. Roden, M.F. Ali, T. Yang, and M.S. Wathen. 2005. Images in cardiovascular medicine. Himalayan T waves in the congenital long-QT syndrome. *Circulation*. 111:e161. <http://dx.doi.org/10.1161/01.CIR.0000159092.92366.CD>
- Despa, S., J. Kockskämper, L.A. Blatter, and D.M. Bers. 2004. Na/K pump-induced [Na]<sup>(i)</sup> gradients in rat ventricular myocytes measured with two-photon microscopy. *Biophys. J.* 87:1360–1368. <http://dx.doi.org/10.1529/biophysj.103.037895>
- Di Benedetto, G., A. Zoccarato, V. Lissandron, A. Terrin, X. Li, M.D. Houslay, G.S. Baillie, and M. Zaccolo. 2008. Protein kinase A type I and type II define distinct intracellular signaling compartments. *Circ. Res.* 103:836–844. <http://dx.doi.org/10.1161/CIRCRESAHA.108.174813>
- DiPilato, L.M., X. Cheng, and J. Zhang. 2004. Fluorescent indicators of cAMP and Epac activation reveal differential dynamics of cAMP signaling within discrete subcellular compartments. *Proc. Natl. Acad. Sci. USA*. 101:16513–16518. <http://dx.doi.org/10.1073/pnas.0405973101>
- Dworkin, M., and K.H. Keller. 1977. Solubility and diffusion coefficient of adenosine 3':5'-monophosphate. *J. Biol. Chem.* 252:864–865.
- Feinstein, W.P., B. Zhu, S.J. Leavesley, S.L. Sayner, and T.C. Rich. 2012. Assessment of cellular mechanisms contributing to cAMP compartmentalization in pulmonary microvascular endothelial cells. *Am. J. Physiol. Cell Physiol.* 302:C839–C852. <http://dx.doi.org/10.1152/ajpcell.00361.2011>
- Fischmeister, R., and M. Horackova. 1983. Variation of intracellular  $\text{Ca}^{2+}$  following  $\text{Ca}^{2+}$  current in heart. A theoretical study of ionic diffusion inside a cylindrical cell. *Biophys. J.* 41:341–348.
- Francis, S.H., M.A. Blount, and J.D. Corbin. 2011. Mammalian cyclic nucleotide phosphodiesterases: molecular mechanisms and physiological functions. *Physiol. Rev.* 91:651–690. <http://dx.doi.org/10.1152/physrev.00030.2010>
- Hanoune, J., and N. Defer. 2001. Regulation and role of adenylyl cyclase isoforms. *Annu. Rev. Pharmacol. Toxicol.* 41:145–174. <http://dx.doi.org/10.1146/annurev.pharmtox.41.1.145>
- Hayes, J.S., L.L. Brunton, J.H. Brown, J.B. Reese, and S.E. Mayer. 1979. Hormonally specific expression of cardiac protein kinase activity. *Proc. Natl. Acad. Sci. USA*. 76:1570–1574. <http://dx.doi.org/10.1073/pnas.76.4.1570>
- Hayes, J.S., L.L. Brunton, and S.E. Mayer. 1980. Selective activation of particulate cAMP-dependent protein kinase by isoproterenol and prostaglandin E1. *J. Biol. Chem.* 255:5113–5119.
- Heijman, J., P.G. Volders, R.L. Westra, and Y. Rudy. 2011. Local control of  $\beta$ -adrenergic stimulation: Effects on ventricular myocyte electrophysiology and  $\text{Ca}^{2+}$ -transient. *J. Mol. Cell. Cardiol.* 50:863–871. <http://dx.doi.org/10.1016/j.yjmcc.2011.02.007>
- Iancu, R.V., S.W. Jones, and R.D. Harvey. 2007. Compartmentation of cAMP signaling in cardiac myocytes: a computational study. *Biophys. J.* 92:3317–3331. <http://dx.doi.org/10.1529/biophysj.106.095356>
- Iancu, R.V., G. Ramamurthy, S. Warriar, V.O. Nikolaev, M.J. Lohse, S.W. Jones, and R.D. Harvey. 2008. Cytoplasmic cAMP concentrations in intact cardiac myocytes. *Am. J. Physiol. Cell Physiol.* 295:C414–C422. <http://dx.doi.org/10.1152/ajpcell.00038.2008>



- Illaste, A., M. Laasmaa, P. Peterson, and M. Vendelin. 2012. Analysis of molecular movement reveals latticelike obstructions to diffusion in heart muscle cells. *Biophys. J.* 102:739–748. <http://dx.doi.org/10.1016/j.bpj.2012.01.012>
- Jepihhina, N., N. Beraud, M. Sepp, R. Birkedal, and M. Vendelin. 2011. Permeabilized rat cardiomyocyte response demonstrates intracellular origin of diffusion obstacles. *Biophys. J.* 101:2112–2121. <http://dx.doi.org/10.1016/j.bpj.2011.09.025>
- Jurevicius, J., and R. Fischmeister. 1996. cAMP compartmentation is responsible for a local activation of cardiac Ca<sup>2+</sup> channels by beta-adrenergic agonists. *Proc. Natl. Acad. Sci. USA.* 93:295–299. <http://dx.doi.org/10.1073/pnas.93.1.295>
- Kapiloff, M.S., M. Rigatti, and K.L. Dodge-Kafka. 2014. Perspectives on: Cyclic nucleotide microdomains and signaling specificity: Architectural and functional roles of A kinase-anchoring proteins in cAMP microdomains. *J. Gen. Physiol.* 143:9–15.
- Karpen, J.W. 2014. Perspectives on: Cyclic nucleotide microdomains and signaling specificity. *J. Gen. Physiol.* 143:5–7.
- Leroy, J., A. Abi-Gerges, V.O. Nikolaev, W. Richter, P. Lechêne, J.L. Mazet, M. Conti, R. Fischmeister, and G. Vandecasteele. 2008. Spatiotemporal dynamics of beta-adrenergic cAMP signals and L-type Ca<sup>2+</sup> channel regulation in adult rat ventricular myocytes: role of phosphodiesterases. *Circ. Res.* 102:1091–1100. <http://dx.doi.org/10.1161/CIRCRESAHA.107.167817>
- Li, C., P.C. Krishnamurthy, H. Penmatsa, K.L. Marrs, X.Q. Wang, M. Zaccolo, K. Jalink, M. Li, D.J. Nelson, J.D. Schuetz, and A.P. Naren. 2007. Spatiotemporal coupling of cAMP transporter to CFTR chloride channel function in the gut epithelia. *Cell.* 131:940–951. <http://dx.doi.org/10.1016/j.cell.2007.09.037>
- Lim, C.J., K.H. Kain, E. Tkachenko, L.E. Goldfinger, E. Gutierrez, M.D. Allen, A. Groisman, J. Zhang, and M.H. Ginsberg. 2008. Integrin-mediated protein kinase A activation at the leading edge of migrating cells. *Mol. Biol. Cell.* 19:4930–4941. <http://dx.doi.org/10.1091/mbc.E08-06-0564>
- Luby-Phelps, K., D.L. Taylor, and F. Lanni. 1986. Probing the structure of cytoplasm. *J. Cell Biol.* 102:2015–2022. <http://dx.doi.org/10.1083/jcb.102.6.2015>
- Mongillo, M., T. McSorley, S. Evellin, A. Sood, V. Lissandron, A. Terrin, E. Huston, A. Hannawacker, M.J. Lohse, T. Pozzan, et al. 2004. Fluorescence resonance energy transfer-based analysis of cAMP dynamics in live neonatal rat cardiac myocytes reveals distinct functions of compartmentalized phosphodiesterases. *Circ. Res.* 95:67–75. <http://dx.doi.org/10.1161/01.RES.0000134629.84732.11>
- Neves, S.R., P. Tsokas, A. Sarkar, E.A. Grace, P. Rangamani, S.M. Taubenfeld, C.M. Alberini, J.C. Schaff, R.D. Blitzer, I.I. Moraru, and R. Iyengar. 2008. Cell shape and negative links in regulatory motifs together control spatial information flow in signaling networks. *Cell.* 133:666–680. <http://dx.doi.org/10.1016/j.cell.2008.04.025>
- Nikolaev, V.O., M. Bünemann, L. Hein, A. Hannawacker, and M.J. Lohse. 2004. Novel single chain cAMP sensors for receptor-induced signal propagation. *J. Biol. Chem.* 279:37215–37218. <http://dx.doi.org/10.1074/jbc.C400302200>
- Nikolaev, V.O., M. Bünemann, E. Schmitteckert, M.J. Lohse, and S. Engelhardt. 2006. Cyclic AMP imaging in adult cardiac myocytes reveals far-reaching beta1-adrenergic but locally confined beta2-adrenergic receptor-mediated signaling. *Circ. Res.* 99:1084–1091. <http://dx.doi.org/10.1161/01.RES.0000250046.69918.d5>
- Nikolaev, V.O., A. Moshkov, A.R. Lyon, M. Miragoli, P. Novak, H. Paur, M.J. Lohse, Y.E. Korchev, S.E. Harding, and J. Gorelik. 2010. Beta2-adrenergic receptor redistribution in heart failure changes cAMP compartmentation. *Science.* 327:1653–1657. <http://dx.doi.org/10.1126/science.1185988>
- Oliveira, R.F., A. Terrin, G. Di Benedetto, R.C. Cannon, W. Koh, M. Kim, M. Zaccolo, and K.T. Blackwell. 2010. The role of type 4 phosphodiesterases in generating microdomains of cAMP: large scale stochastic simulations. *PLoS ONE.* 5:e11725. <http://dx.doi.org/10.1371/journal.pone.0011725>
- Ostrom, R.S., C. Gregorian, R.M. Drenan, Y. Xiang, J.W. Regan, and P.A. Insel. 2001. Receptor number and caveolar co-localization determine receptor coupling efficiency to adenylyl cyclase. *J. Biol. Chem.* 276:42063–42069. <http://dx.doi.org/10.1074/jbc.M105348200>
- Parfenov, A.S., V. Salnikov, W.J. Lederer, and V. Lukanenko. 2006. Aqueous diffusion pathways as a part of the ventricular cell ultrastructure. *Biophys. J.* 90:1107–1119. <http://dx.doi.org/10.1529/biophysj.105.071787>
- Poppe, H., S.D. Rybalkin, H. Rehmann, T.R. Hinds, X.B. Tang, A.E. Christensen, F. Schwede, H.G. Genieser, J.L. Bos, S.O. Doskeland, et al. 2008. Cyclic nucleotide analogs as probes of signaling pathways. *Nat. Methods.* 5:277–278. <http://dx.doi.org/10.1038/nmeth0408-277>
- Rich, T.C., K.A. Fagan, H. Nakata, J. Schaack, D.M. Cooper, and J.W. Karpen. 2000. Cyclic nucleotide-gated channels colocalize with adenylyl cyclase in regions of restricted cAMP diffusion. *J. Gen. Physiol.* 116:147–162. <http://dx.doi.org/10.1085/jgp.116.2.147>
- Rich, T.C., K.A. Fagan, T.E. Tse, J. Schaack, D.M. Cooper, and J.W. Karpen. 2001. A uniform extracellular stimulus triggers distinct cAMP signals in different compartments of a simple cell. *Proc. Natl. Acad. Sci. USA.* 98:13049–13054. <http://dx.doi.org/10.1073/pnas.221381398>
- Rich, T.C., W. Xin, C. Mehats, K.A. Hassell, L.A. Piggott, X. Le, J.W. Karpen, and M. Conti. 2007. Cellular mechanisms underlying prostaglandin-induced transient cAMP signals near the plasma membrane of HEK-293 cells. *Am. J. Physiol. Cell Physiol.* 292:C319–C331. <http://dx.doi.org/10.1152/ajpcell.00121.2006>
- Rich, T.C., K.J. Webb, and S.J. Leavesley. 2014. Perspectives on: Cyclic nucleotide microdomains and signaling specificity: Can we decipher the information content contained within cyclic nucleotide signals? *J. Gen. Physiol.* 143:17–27.
- Rochais, F., G. Vandecasteele, F. Lefebvre, C. Lugnier, H. Lum, J.L. Mazet, D.M. Cooper, and R. Fischmeister. 2004. Negative feedback exerted by cAMP-dependent protein kinase and cAMP phosphodiesterase on subsarcolemmal cAMP signals in intact cardiac myocytes: an in vivo study using adenovirus-mediated expression of CNG channels. *J. Biol. Chem.* 279:52095–52105. <http://dx.doi.org/10.1074/jbc.M405697200>
- Rochais, F., A. Abi-Gerges, K. Horner, F. Lefebvre, D.M. Cooper, M. Conti, R. Fischmeister, and G. Vandecasteele. 2006. A specific pattern of phosphodiesterases controls the cAMP signals generated by different Gs-coupled receptors in adult rat ventricular myocytes. *Circ. Res.* 98:1081–1088. <http://dx.doi.org/10.1161/01.RES.0000218493.09370.8e>
- Rybin, V.O., X. Xu, M.P. Lisanti, and S.F. Steinberg. 2000. Differential targeting of beta-adrenergic receptor subtypes and adenylyl cyclase to cardiomyocyte caveolae. A mechanism to functionally regulate the cAMP signaling pathway. *J. Biol. Chem.* 275:41447–41457. <http://dx.doi.org/10.1074/jbc.M006951200>
- Sample, V., L.M. DiPilato, J.H. Yang, Q. Ni, J.J. Saucerman, and J. Zhang. 2012. Regulation of nuclear PKA revealed by spatiotemporal manipulation of cyclic AMP. *Nat. Chem. Biol.* 8:375–382. <http://dx.doi.org/10.1038/nchembio.799>
- Saucerman, J.J., and A.D. McCulloch. 2006. Cardiac beta-adrenergic signaling: from subcellular microdomains to heart failure. *Ann. NY Acad. Sci.* 1080:348–361. <http://dx.doi.org/10.1196/annals.1380.026>
- Saucerman, J.J., L.L. Brunton, A.P. Michailova, and A.D. McCulloch. 2003. Modeling beta-adrenergic control of cardiac myocyte contractility in silico. *J. Biol. Chem.* 278:47997–48003. <http://dx.doi.org/10.1074/jbc.M308362200>
- Saucerman, J.J., S.N. Healy, M.E. Belik, J.L. Puglisi, and A.D. McCulloch. 2004. Proarrhythmic consequences of a KCNQ1

- AKAP-binding domain mutation: computational models of whole cells and heterogeneous tissue. *Circ. Res.* 95:1216–1224. <http://dx.doi.org/10.1161/01.RES.0000150055.06226.4e>
- Saucerman, J.J., J. Zhang, J.C. Martin, L.X. Peng, A.E. Stenbit, R.Y. Tsien, and A.D. McCulloch. 2006. Systems analysis of PKA-mediated phosphorylation gradients in live cardiac myocytes. *Proc. Natl. Acad. Sci. USA.* 103:12923–12928. <http://dx.doi.org/10.1073/pnas.0600137103>
- Sayner, S.L., D.W. Frank, J. King, H. Chen, J. VandeWaa, and T. Stevens. 2004. Paradoxical cAMP-induced lung endothelial hyperpermeability revealed by *Pseudomonas aeruginosa* ExoY. *Circ. Res.* 95:196–203. <http://dx.doi.org/10.1161/01.RES.0000134922.25721.d9>
- Sayner, S.L., M. Alexeyev, C.W. Dessauer, and T. Stevens. 2006. Soluble adenylyl cyclase reveals the significance of cAMP compartmentation on pulmonary microvascular endothelial cell barrier. *Circ. Res.* 98:675–681. <http://dx.doi.org/10.1161/01.RES.0000209516.84815.3e>
- Steinberg, S.F., and L.L. Brunton. 2001. Compartmentation of G protein-coupled signaling pathways in cardiac myocytes. *Annu. Rev. Pharmacol. Toxicol.* 41:751–773. <http://dx.doi.org/10.1146/annurev.pharmtox.41.1.751>
- Terrin, A., G. Di Benedetto, V. Pertegato, Y.F. Cheung, G. Baillie, M.J. Lynch, N. Elvassore, A. Prinz, F.W. Herberg, M.D. Houslay, and M. Zaccolo. 2006. PGE(1) stimulation of HEK293 cells generates multiple contiguous domains with different [cAMP]: role of compartmentalized phosphodiesterases. *J. Cell Biol.* 175:441–451. <http://dx.doi.org/10.1083/jcb.200605050>
- Willoughby, D., and D.M. Cooper. 2007. Organization and Ca<sup>2+</sup> regulation of adenylyl cyclases in cAMP microdomains. *Physiol. Rev.* 87:965–1010. <http://dx.doi.org/10.1152/physrev.00049.2006>
- Xie, M., T.C. Rich, C. Scheitrum, M. Conti, and W. Richter. 2011. Inactivation of multidrug resistance proteins disrupts both cellular extrusion and intracellular degradation of cAMP. *Mol. Pharmacol.* 80:281–293. <http://dx.doi.org/10.1124/mol.111.071134>
- Yang, J.H., and J.J. Saucerman. 2011. Computational models reduce complexity and accelerate insight into cardiac signaling networks. *Circ. Res.* 108:85–97. <http://dx.doi.org/10.1161/CIRCRESAHA.110.223602>
- Zaccolo, M., and T. Pozzan. 2002. Discrete microdomains with high concentration of cAMP in stimulated rat neonatal cardiac myocytes. *Science.* 295:1711–1715. <http://dx.doi.org/10.1126/science.1069982>
- Zaccolo, M., F. De Giorgi, C.Y. Cho, L. Feng, T. Knapp, P.A. Negulescu, S.S. Taylor, R.Y. Tsien, and T. Pozzan. 2000. A genetically encoded, fluorescent indicator for cyclic AMP in living cells. *Nat. Cell Biol.* 2:25–29. <http://dx.doi.org/10.1038/71345>